180D Lab Report 1

David Llewellyn Smith

October 28, 2024

1 Introduction

The main objective of this experiment was to measure the speed of sound in air using resonant modes in a rectangular and a cylindrical enclosure. Measurements of the first 33 rectangular modes and 17 cylindrical modes were used to calculate the speed of sound. This was accomplished by using a speaker driven by a function generator. Then, maps of the amplitude of pressure oscillations were created for each dimension in each enclosure in order to understand the shape of sound waves.

2 Theory

We begin with the fundamental equations governing a gaseous fluid: conservation of mass (1), Euler's equation (2), and the equation of state for an ideal gas (3).

$$\frac{\partial \rho}{\partial t} + \boldsymbol{\nabla} \cdot (\rho \mathbf{u}) = 0. \tag{1}$$

$$\frac{\partial \mathbf{u}}{\partial t} + (\mathbf{u} \cdot \boldsymbol{\nabla})\mathbf{u} = -\frac{\boldsymbol{\nabla} p}{\rho} \tag{2}$$

$$p = \frac{\rho R T}{M} \tag{3}$$

where p is the pressure, ρ is the density, $\mathbf{u}$ is the velocity field, $R = 8.31 \frac{J}{molK}$ is the gas constant, T is the temperature, and M is the total mass. Then, linearizing under the assumption v << c, the speed of sound, we get the wave equation:

$$\nabla^2 p - \frac{1}{c^2}\frac{\partial^2 p}{\partial t^2} = 0 \tag{4}$$

Assuming solutions of the form

$$p = A e^{-i\omega t}\cos(k_x x)\cos(k_y y)\cos(k_z z), \tag{5}$$

then resonant modes imply the boundary conditions

$$\left.\frac{\partial p}{\partial x}\right|_{x=0,L_x} = 0, \quad \left.\frac{\partial p}{\partial y}\right|_{x=0,L_y} = 0, \quad \left.\frac{\partial p}{\partial z}\right|_{x=0,L_z} = 0. \tag{6}$$

This allows us to derive the resonant frequencies in a rectangular box:

$$f_{xyz} = \frac{c}{2}\sqrt{\frac{n_x^2}{L_x^2} + \frac{n_y^2}{L_y^2} + \frac{n_z^2}{L_z^2}}. \tag{7}$$

For a cylindrical box, we use the Laplacian in cylindrical coordinates

$$\nabla^2 = \frac{1}{r}\frac{\partial}{\partial r}\left(r\frac{\partial}{\partial r}\right) + \frac{1}{r^2}\frac{\partial^2}{\partial \theta^2} + \frac{\partial^2}{\partial z^2} \tag{8}$$

and obtain

$$f_{mnz} = \frac{c}{2}\sqrt{\frac{{j'_{mn}}^2}{\pi^2 R^2} + \frac{n_z^2}{L_z^2}} \tag{9}$$

with the extrema points of the Bessel function j' given on page 7 of the lab handout [1].

3 Experimental Setup

3.1 Materials

The experiment was performed using a rectangular box with dimensions of 20.3 ± 0.05 cm by 16.1 ± 0.05 cm by 14.0 ± 0.05 cm, a cylindrical box of radius 12.1 ± 0.05 cm and height 4.6 ± 0.05 cm, a speaker, a microphone, function generator, and an oscilloscope. The rectangular box had three holes in it and an open face. The holes were located at the center of one face, near the corner on that same face, and near an edge on that face. The cylindrical box had an open bottom and a movable hole located on top. The data was analyzed using LabView and Matlab.

3.2 Frequency Sweep

The first part of the experiment involved sweeping from a frequency of 500 Hertz to 5 kiloHertz over a span of two seconds in order to identify the resonant modes of the boxes. This was performed six times, three times for each box. For the rectangular box, the microphone was inserted into each of the three holes on the side. For the cylindrical box, the microphone was inserted into the hole on top of the box and then placed at the center, on the edge, and then rotated 90^{o} to another edge. Each box was placed with their open face on a flat surface with a hole for the speaker. An FFT was performed on the results of the process to transform the data into frequency space.

3.3 Pressure Maps

The next part of the experiment involved taking voltage measurements from the microphone along each axis in order to map out the nodes of the resonant frequencies. Two resonant frequencies were chosen for each box. For the rectangular box, the microphone was placed in the hole in the center of the side. Measurements were taken by shifting the box 5cm at a time in all three directions. Then, measurements were taken for the cylindrical box by rotating it 5 degrees at a time and then by moving the location of the microphone along the diameter 5cm at a time. The microphone was attached to an oscilloscope which read the intensity of the voltage coming into the microphone.

4 Data/Analysis

4.1 Speed of Sound

In Figure 1 are plotted the power spectral densities for each of the three sweeps using the rectangular box. The resonance frequencies are marked with orange dots and represented in Table 1 (if less than the 4,0,0 mode). Some modes are too close together to tell apart so there are only 31 distinct observed modes instead of the expected 33. The mode numbers were determined by calculating expected frequencies using (7) with an estimated speed of sound value of 345 m/s. Comparison of the three spectra shows that some frequencies don't appear in every spectra, which is a consequence of mode elimination and the geometry of where the speaker and microphone were placed. This also gives uncertainties for the frequencies with multiple measured values. For those only observed once, I've used the width at half-maximum. Using the observed frequencies, we can use (7) to calculate the speed of sound in the box for each mode. Those results are column 3 of Table 1 and are plotted in Figure 2. The mean of the values is 345.005 m/s and the median is 344.97 m/s. Analysis of the accuracy of these numbers is found in Section 5 but the proximity to the estimated value used at the beginning is encouraging.

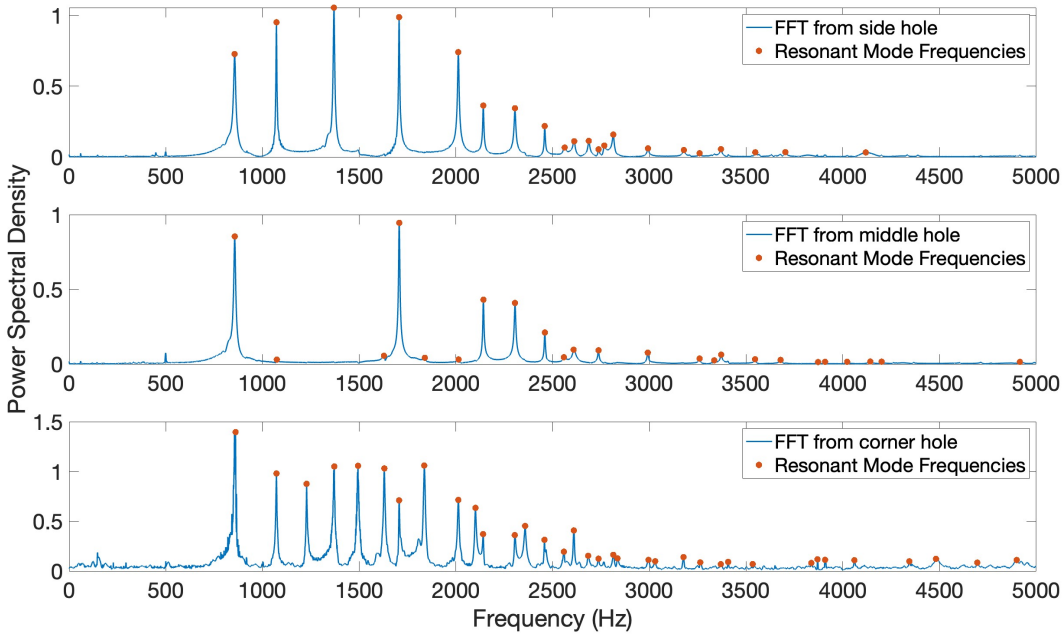

Figure 1: FFT results for the rectangular box

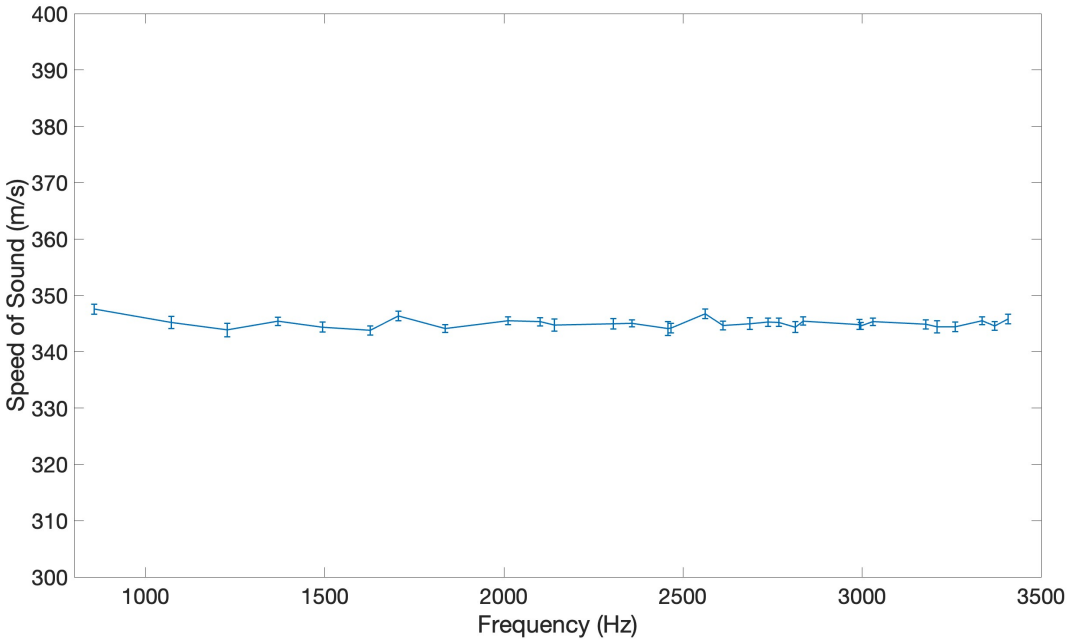

Figure 2: Measured Speed of Sound

Mode	Expected F (Hz)	Observed F (Hz)	Speed of Sound (m/s)
1,0,0	849.8	856	347.5±0.9
0,1,0	1071.4	1072	345.2±1.1
0,0,1	1232.1	1228	343.8±1.2
1,1,0	1367	1369	345.3±0.7
1,0,1	1496.7	1494	344.4±0.9
0,1,1	1632.8	1627	343.8±0.8
2,0,0	1699.5	1706	346.3±0.9
1,1,1	1840.7	1836	344.1±0.7
2,1,0	2009.1	2012	345.5±0.7
2,0,1	2099.2	2101	345.3±0.7
0,2,0	2142.9	2141	344.7±1.1
1,2,0	2305.2	2305	345.0±0.9
2,1,1	2356.8	2357	345.0±0.6
0,0,2	2464.3	2458	344.1±1.2
0,2,1	2471.8	2466	344.2±0.9
3,0,0	2549.3	2562	346.7±0.9
1,0,2	2606.7	Too Faint	
1,2,1	2613.8	2611	344.6±0.8
0,1,2	2687.1	2687	344.6±1.1
2,2,0	2735	2737	345.0±0.7
3,1,0	2765.3	2767	345.3±0.7
1,1,2	2818.3	2813	345.2±1.0
3,0,1	2831.4	2835	344.4±0.7
2,0,2	2993.5	2992	345.4±0.9
2,2,1	2999.7	2996	344.8±0.6
3,1,1	3027.4	3030	344.6±0.7
2,1,2	3179.5	3178	345.3±0.8
0,3,0	3214.3	3209	344.8±1.1
0,2,2	3265.7	3260	344.4±0.8
1,3,0	3324.7	Too faint	
3,2,0	3330.3	3335	345.5±0.7
1,2,2	3374.4	3370	344.5±0.8
4,0,0	3399	3407	345.8±0.9

Table 1: Observed Resonances in Figures 1-3

In Figure 3, we see the results from the trials using the cylindrical box. The first placed the microphone in the middle of the cylinder, the second placed it on the edge, and and the third rotated it 90 degrees around the edge. Only the most prominent modes are plotted but all 15 are included in Table 2. The speed of sound was calculated for each frequency in the third column and plotted in Figure 4. The mean is 345.3 m/s and the median is 345.5.

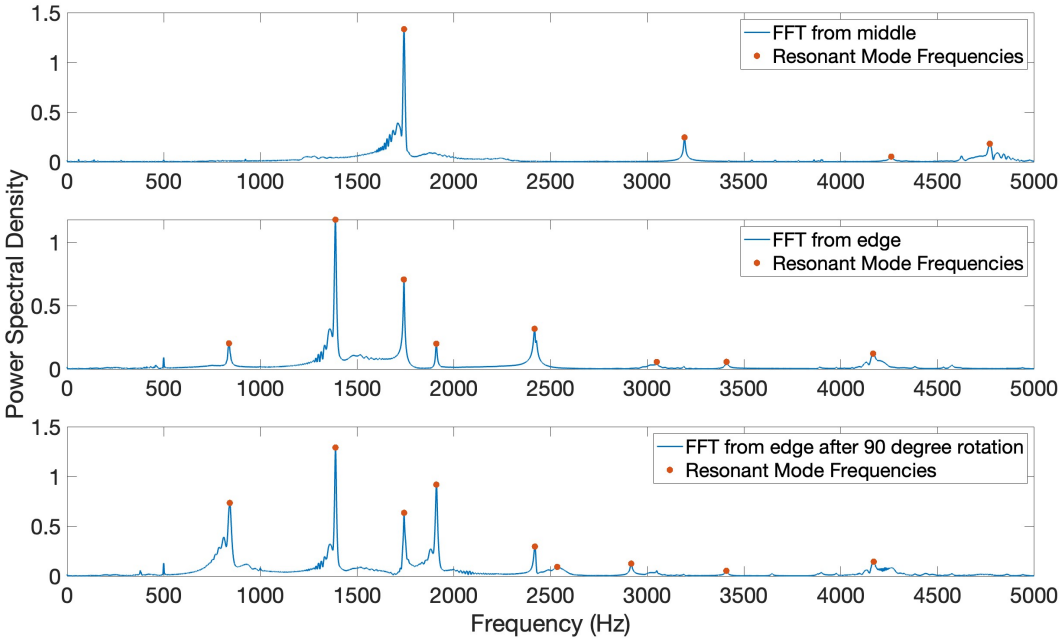

Figure 3: FFT results for the cylindrical box

Mode	Expected F (Hz)	Observed F (Hz)	Speed of Sound (m/s)
1,1,0	835.5	837.1	345.7±1.4
2,1,0	1386	1387.6	345.4±1.4
0,2,0	1738.8	1741.2	345.5±1.4
3,1,0	1906.5	1909.3	345.5±1.4
4,1,0	2413.1	2416.5	345.5±1.4
1,2,0	2419.3	2425.8	345.9±1.4
2,2,0	3043.2	3048.5	345.6±1.4
0,3,0	3183.6	3188.7	345.6±1.4
3,2,0	3637.2	3644.3	345.7±1.4
1,1,1	3842.0	3843.0	345.1±0.1
1,3,0	3873.7	3890.7	346.5±1.4
2,1,1	3997.9	3977.3	343.2±0.2
0,2,1	4133.5	4132.0	344.9±0.3
3,1,1	4206.8	4205.2	344.9±0.3
4,2,0	4212.2	4213.4	345.1±1.4

Table 2: Observed Resonances in Figure 3

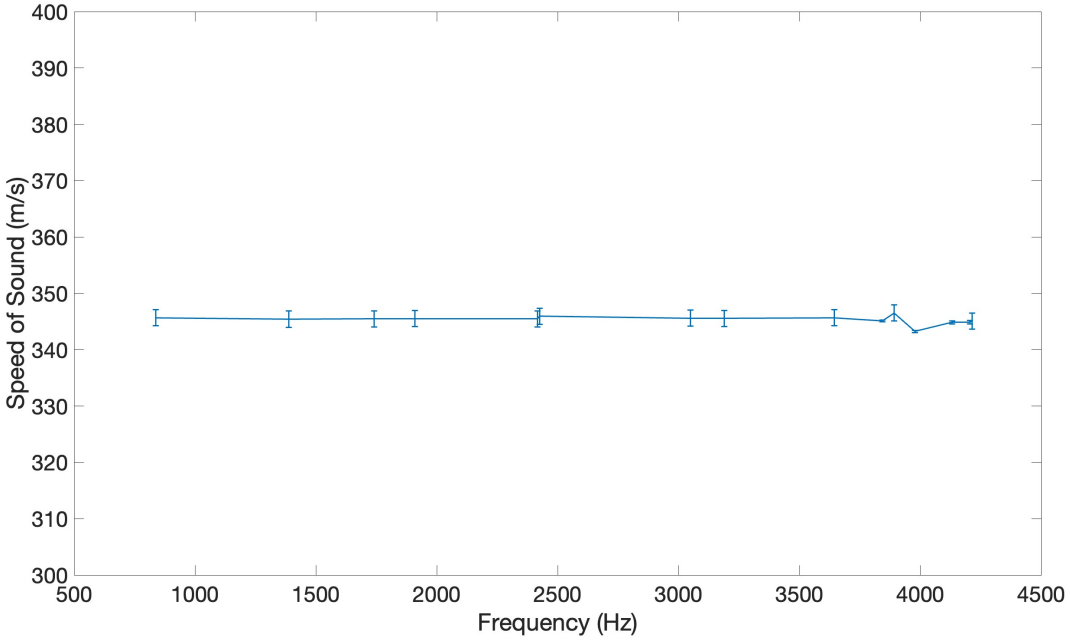

Figure 4: Speed of sound for cylindrical modes

4.2 Pressure Maps

Figures 5-14 are the ten pressure maps that were created. Two frequencies were chosen for both the rectangular box and the cylindrical box. For the rectangular box, they were the (1,1,1) mode, about 1840 Hz, and the (2,1,1) mode, about 2360 Hz. For the cylindrical box, they were the (1,1,0) mode, about 840 Hz, and the (4,1,0) mode, about 2415 Hz. For some of the rectangular pressure maps, I plotted an approximate fit using equation 5.

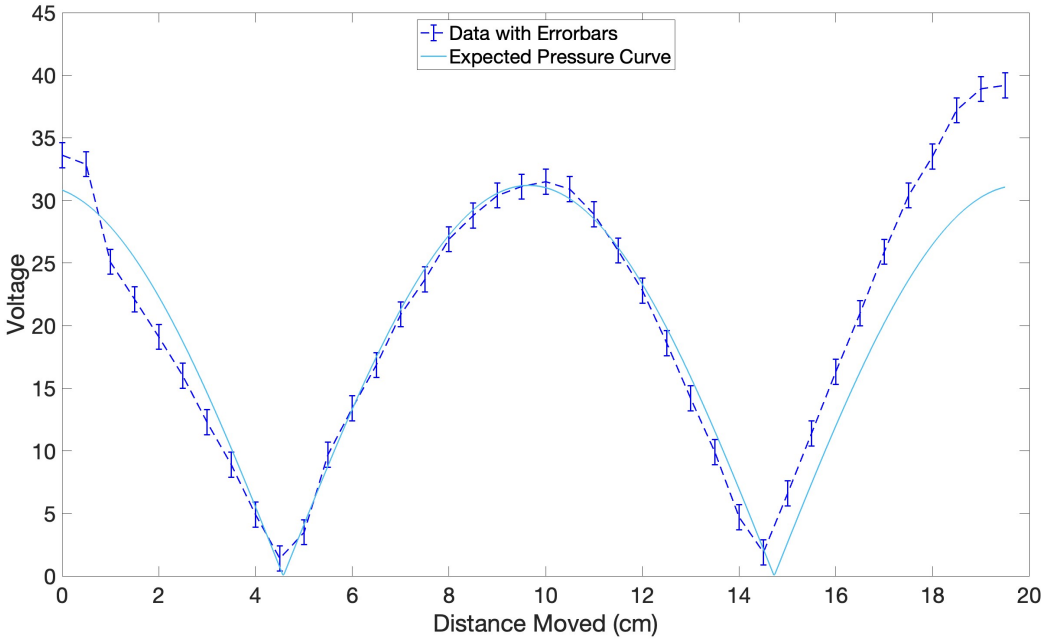

Figure 5: Pressure map in the x-direction for the (2,1,1) mode at 2360 Hz. The points with errorbars indicate the data, connected by a dashed line as a visual aid, and the solid line is an approximate fit using the theory in equation (5)

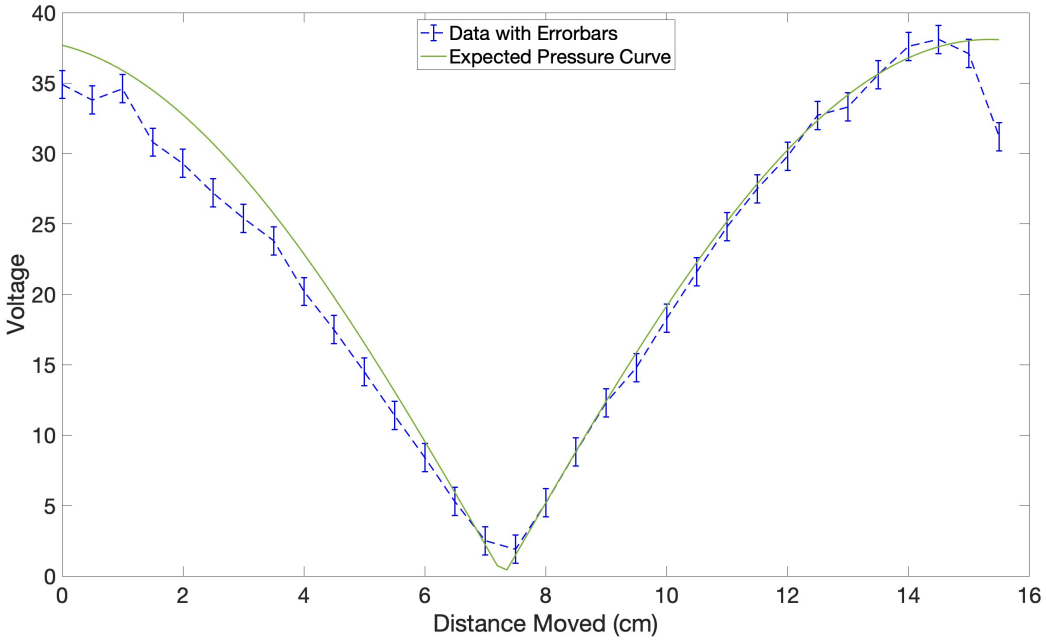

Figure 6: As in Figure 5 but in the y-direction.

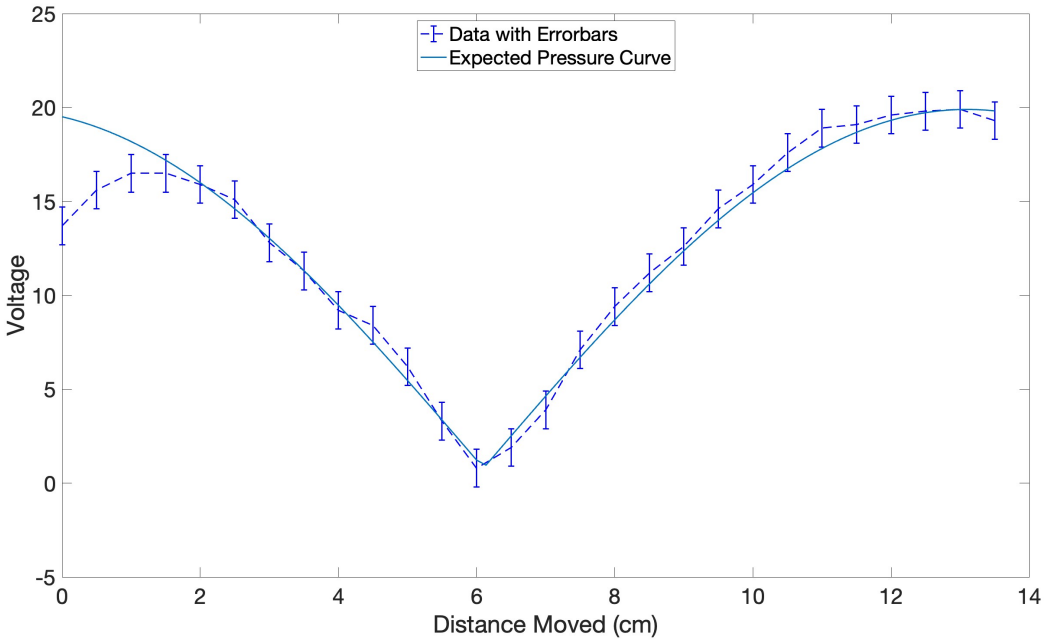

Figure 7: As in Figure 5 but in the z-direction.

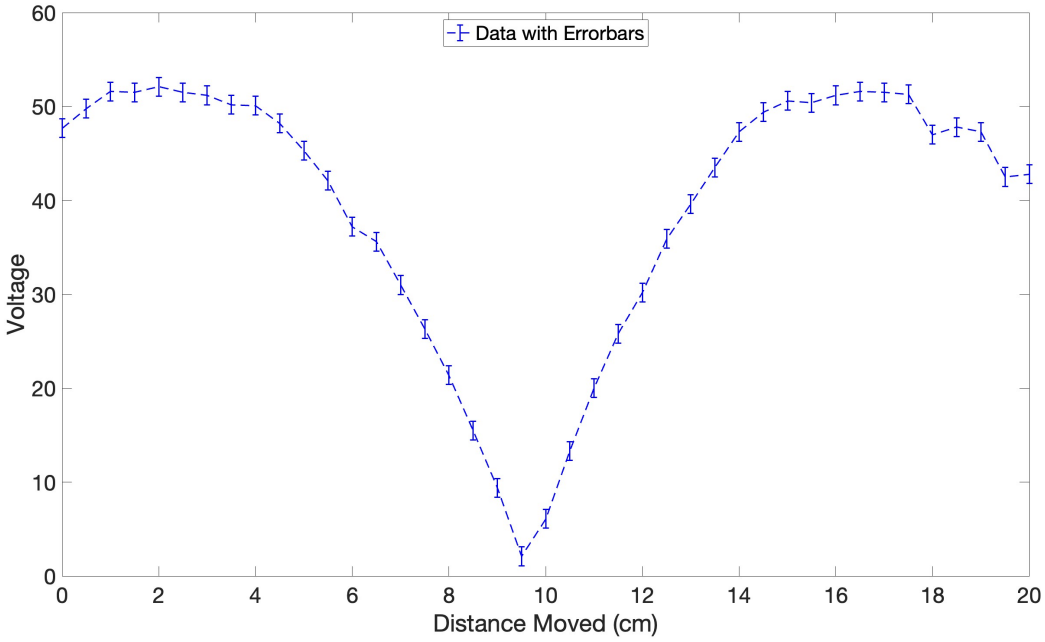

Figure 8: As in Figure 5 but using the (1,1,1) mode with frequency 1840 Hz.

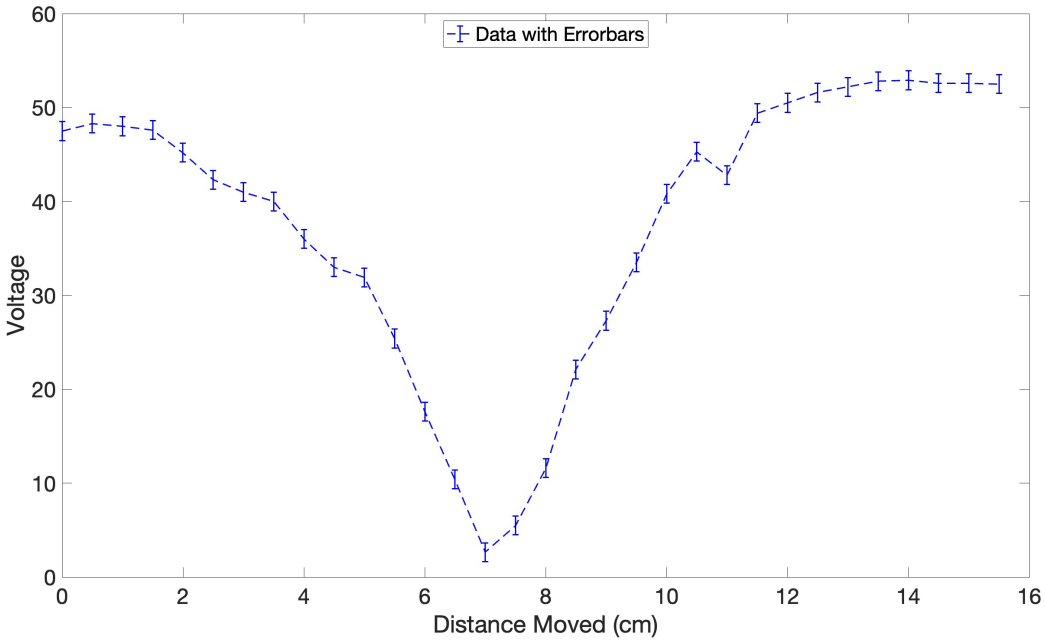

Figure 9: As in Figure 8 but in the y-direction.

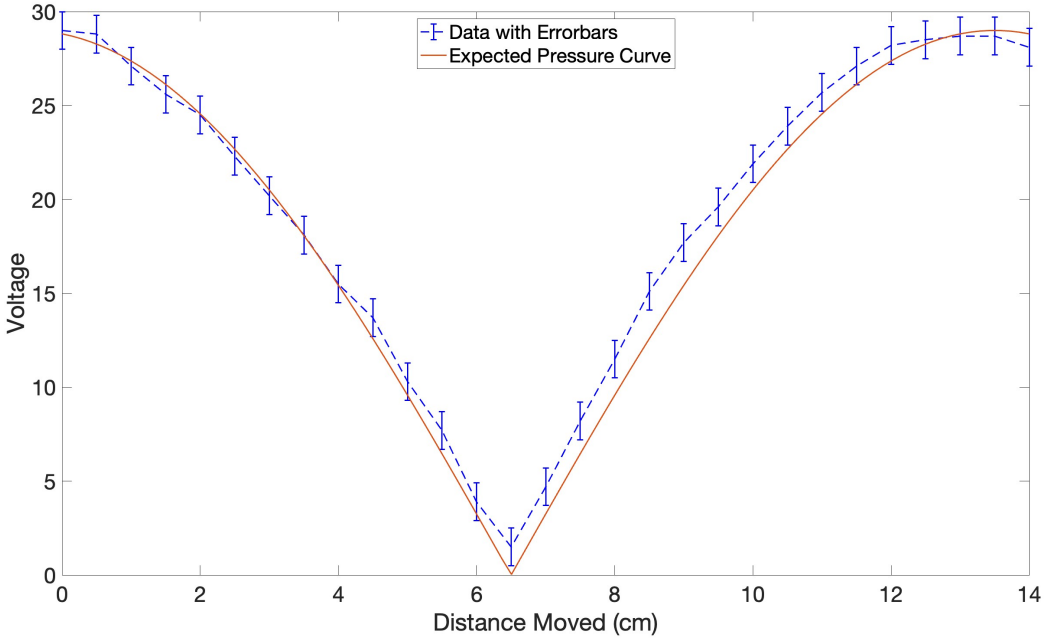

Figure 10: As in Figure 8 but in the z-direction.

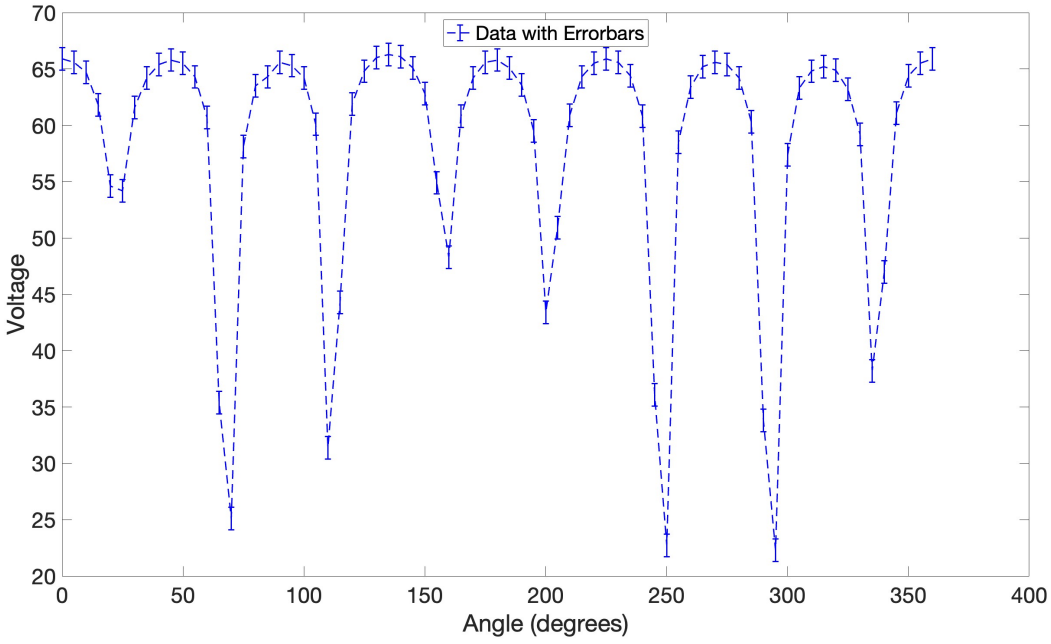

Figure 11: Pressure map around the edge of the cylinder for the (4,1,0) mode at 2420 Hz. The points with errorbars indicate the data, connected by a dashed line as a visual aid.

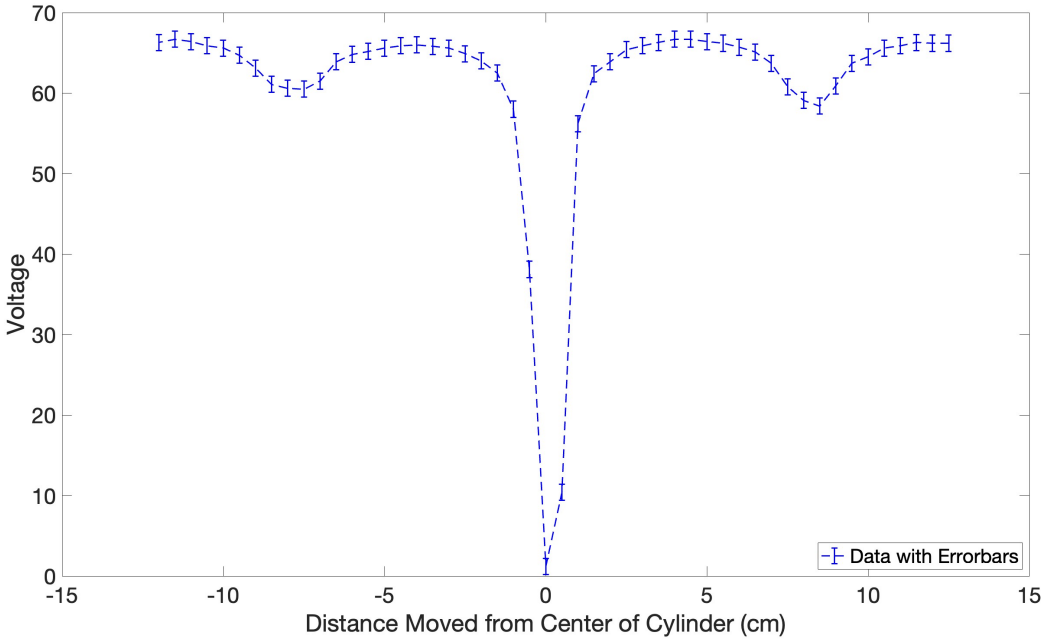

Figure 12: As in Figure 11 but along the diameter of the cylinder.

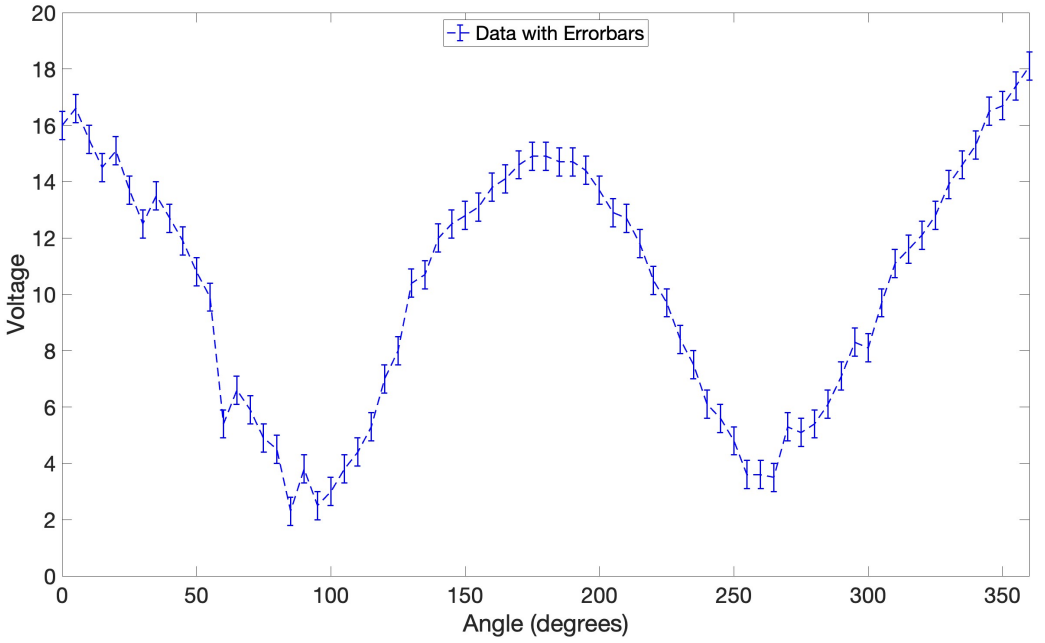

Figure 13: As in Figure 11 but for the (1,1,0) mode at 840 Hz.

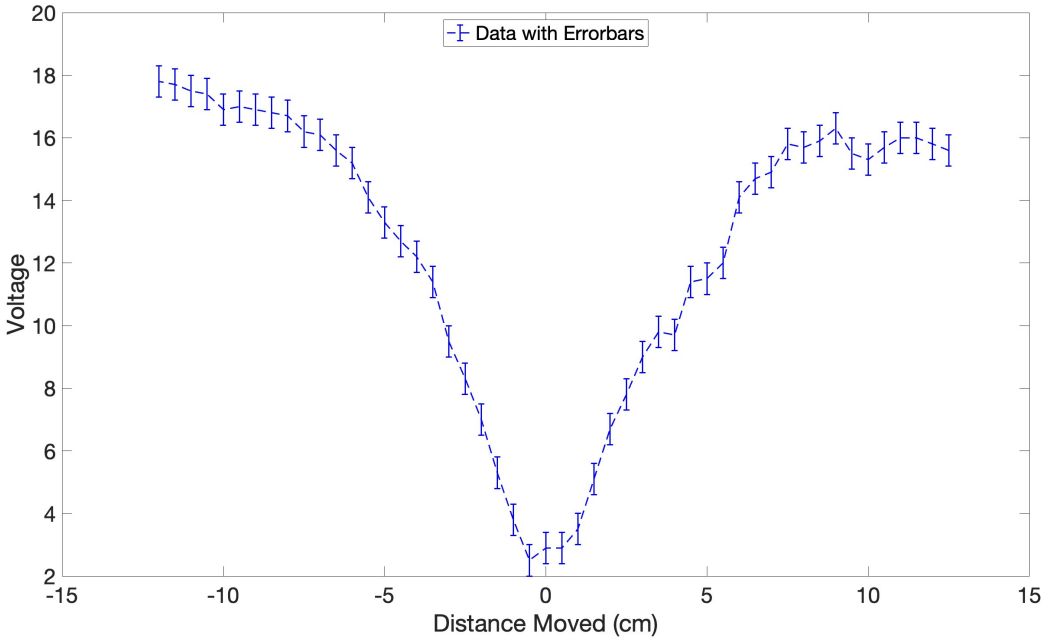

Figure 14: As in Figure 12 but for the (1,1,0) mode at 840 Hz.

5 Error Analysis

In order to gauge the accuracy of our calculations of the speed of sound, we can find it in a different way, using

$$c = \sqrt{\frac{\gamma RT}{M_w}}, \tag{10}$$

where $\gamma = \frac{C_p}{C_v}$ and M_w is the molecular weight of air. We'll define

$$X = h\frac{\text{saturated vapor pressure}}{\text{barometric pressure}} \tag{11}$$

Then, from [1],

$$\begin{aligned} M_w &= (X * 18) + ((1 - X) * ((0.78 * 28) + (0.21 * 32) + (0.01 * 40))) \\ &= 18X + 28.96 - 28.96X = 28.96 - 10.96X \end{aligned} \tag{12}$$

The conditions of the lab during the experiment were $T = 22.5 \pm 1°C$, $h = 58\%$, and $p = 1013.25$ hPa. Using the Tetens equation for the saturated vapor pressure [2], we have

$$\begin{aligned} P &= 0.61078 \exp\left(\frac{17.27T}{T + 237.3}\right) \\ &= 27.25 \text{ hPa} \end{aligned} \tag{13}$$

$$X = h * \frac{27.25}{1013.25} = 0.016 \tag{14}$$

Using

$$C_v = (X * C_v(H_2O)) + ((1 - X) * 2.5 * R) \tag{15}$$

$$C_p = C_v + R \tag{16}$$

we get

$$\gamma = 1.400 \tag{17}$$

$$M_w = 28.96 - 0.16 = 28.79. \tag{18}$$

This allows us to calculate

$$c = \sqrt{\frac{1.400 * 8.31 * 295.65}{0.02879}} = 345.66 \text{ m/s} \tag{19}$$

Given the means of our calculated values before were 345.0 and 345.3 m/s, this is quite encouraging. Uncertainties in the speed of sound were calculated using the uncertainty in our measurements of the dimensions of the box. Using

$$\sigma_c = \sqrt{\left(\frac{\partial c}{\partial L_x}\right)^2 \sigma_{L_x}^2 + \left(\frac{\partial c}{\partial L_y}\right)^2 \sigma_{L_y}^2 + \left(\frac{\partial c}{\partial L_z}\right)^2 \sigma_{L_z}^2} \tag{20}$$

and

$$\sigma_c = \sqrt{\left(\frac{\partial c}{\partial R}\right)^2 \sigma_R^2 + \left(\frac{\partial c}{\partial L_z}\right)^2 \sigma_{L_z}^2} \tag{21}$$

with (for any dimension)

$$\frac{\partial c}{\partial L} = \frac{2fn^2}{L^3\left(\frac{n_x^2}{L_x^2} + \frac{n_y^2}{L_y^2} + \frac{n_z^2}{L_z^2}\right)^{\frac{3}{2}}} \tag{22}$$

and

$$\frac{\partial c}{\partial R} = \frac{2f{j'_{mn}}^2}{R^3\pi^3\left(\frac{{j'_{mn}}^2}{R^2\pi^2} + \frac{n_z^2}{L_z^2}\right)^{\frac{3}{2}}}. \tag{23}$$

These uncertainties are alongside the calculated values of the speed of sound in Tables 1 and 2. Based on Figures 2 and 4 which show the speed of sound to be constant within uncertainty as a function of frequency, we can conclude that the uncertainty of the size of the box did not impact our calculations significantly.

6 Conclusion

We measured the speed of sound using resonances in a box and found a value of about 345 m/s. This aligns with the theoretical calculation using ambient temperature, humidity, and pressure. Pressure maps were created showing the rise and fall of pressure according to its resonances. Within assumed uncertainty, these aligned with their hypothesized shape based on the solution to the pressure wave equation. They could have been better if we had a better way to measure voltage than manually reading it from the screen of the oscilloscope and a more accurate way to move the box than our hands and a ruler. A more automated measurement approach would allow for faster sampling and to better sample the variations at the extrema.

7 References

[1] UCLA Physics 180D, Experiment 1: Room Acoustics.
bruinlearn.ucla.edu/courses/194667/pages/experiment-1-room-acoustics

[2] Tetens, O. 1930. Über einige meteorologische Begriffe. Z. Geophys 6: 297-309